ISSN 0964-6906

HUMAN MOLECULAR GENETICS

Volume 18 Number 9 1 May 2009
www.hmg.oxfordjournals.org

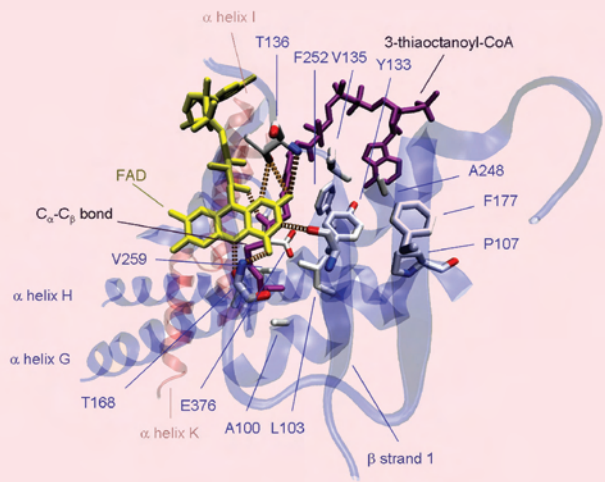

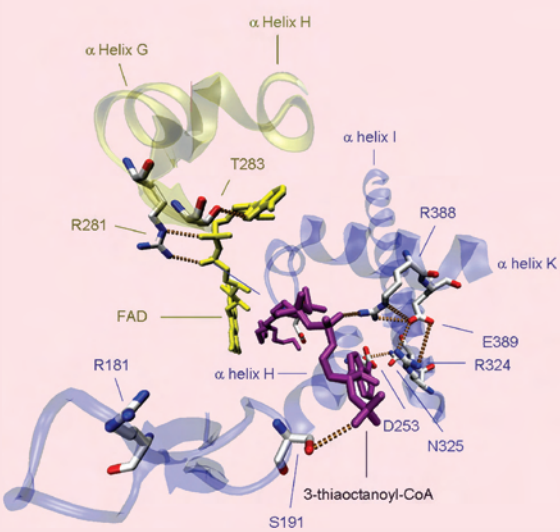

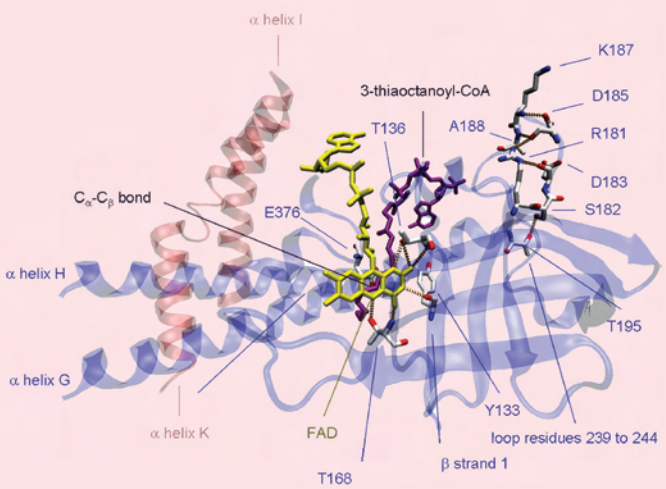

VOLUME 18 NUMBER 9 1 MAY 2009 PAGES 1545–1718 HUMAN MOLECULAR GENETICS OXFORD

Human Molecular Genetics, 2009, Vol. 18, No. 9 ***1612–1623***
doi:10.1093/hmg/ddp079
Advance Access published on February 18, 2009

Protein misfolding is the molecular mechanism underlying MCADD identified in newborn screening

Esther M. Maier[1,†], Søren W. Gersting[1,†], Kristina F. Kemter[1], Johanna M. Jank[1], Maria Reindl[1], Dunja D. Messing[1], Marietta S. Truger[1], Christian P. Sommerhoff[2] and Ania C. Muntau[1,*]

[1]Department of Molecular Pediatrics, Children's Research Center, Dr. von Hauner Children's Hospital, Ludwig-Maximilians-University, Lindwurmstr. 4, Munich 80337, Germany and [2]Department of Clinical Chemistry and Clinical Biochemistry, Ludwig-Maximilians-University, Munich 80336, Germany

Received January 13, 2009; Revised and Accepted February 16, 2009

Newborn screening (NBS) for medium-chain acyl-CoA dehydrogenase deficiency (MCADD) revealed a higher birth prevalence and genotypic variability than previously estimated, including numerous novel missense mutations in the *ACADM* gene. On average, these mutations are associated with milder biochemical phenotypes raising the question about their pathogenic relevance. In this study, we analyzed the impact of 10 *ACADM* mutations identified in NBS (A27V, Y42H, Y133H, R181C, R223G, D241G, K304E, R309K, I331T and R388S) on conformation, stability and enzyme kinetics of the corresponding proteins. Partial to total rescue of aggregation by co-overexpression of GroESL indicated protein misfolding. This was confirmed by accelerated thermal unfolding in all variants, as well as decreased proteolytic stability and accelerated thermal inactivation in most variants. Catalytic function varied from high residual activity to markedly decreased activity or substrate affinity. Mutations mapping to the β-domain of the protein predisposed to severe destabilization. *In silico* structural analyses of the affected amino acid residues revealed involvement in functionally relevant networks. Taken together, our results substantiate the hypothesis of protein misfolding with loss-of-function being the common molecular basis in MCADD. Moreover, considerable structural alterations in all analyzed variants do not support the view that novel mutations found in NBS bear a lower risk of metabolic decompensation than that associated with mutations detected in clinically ascertained patients. Finally, the detailed insight into how *ACADM* missense mutations induce loss of MCAD function may provide guidance for risk assessment and counseling of patients, and in future may assist delineation of novel pharmacological strategies.

INTRODUCTION

Newborn screening (NBS) for medium-chain acyl-CoA dehydrogenase deficiency (MCADD; MIM #201450) by tandem-mass spectrometry has successfully been implemented in many countries worldwide (1). MCADD revealed a notably higher birth prevalence (∼1:15000) than previously estimated (1–3) and nowadays is the disorder most frequently diagnosed in NBS, together with phenylketonuria (4). The disease leads to a defect in mitochondrial β-oxidation of fatty acids. Patients show a decreased ability to withstand catabolic stress and risk coma and death due to hypoketotic hypoglycemia during prolonged fasting or intercurrent illness. In undiagnosed patients, the disorder shows a significant morbidity and mortality. Approximately 20% of patients die during their first metabolic crisis and ∼40% of the survivors show sustained neurological impairment (5–7). Once diagnosed, however, adverse effects can be prevented by avoidance of fasting during episodes of catabolic stress. Thus, MCADD is the disorder thought to most justify early detection by NBS (4).

In patients diagnosed after metabolic decompensation, the mutation K304E (c.985A>G) (*ACADM* gene; OMIM #607008) has been shown to account for 90% of defective alleles (8) and therefore is considered to be a severe mutation associated with a high risk of clinical manifestation (9).

*To whom correspondence should be addressed. Tel: +49 89 5160 2746; Fax: +49 89 5160 7792; Email: ania.muntau@med.uni-muenchen.de
†The authors wish it to be known that, in their opinion, the first two authors should be regarded as joint First Authors.

K304E and few other missense mutations identified in symptomatic patients were previously shown to induce protein misfolding and aggregation (10–17).

MCADD patients identified by NBS show a considerably wider genotypic heterogeneity with the mutation K304E being less prevalent. Numerous novel mutations were unraveled including a second prevalent mutation, Y42H (c.199T>C) (3,18–20). After diagnosis, patients carrying these allelic variants follow disease management plans to avoid metabolic crises. Thus, the natural course of MCADD associated with this new group of mutations is unlikely to be witnessed. On average, these patients express lower disease markers (octanoylcarnitine and related acylcarnitine ratios in blood) than observed in homo- or heterozygosity for K304E (3,18,20). However, the different genotypes show a high variability of values, and it is generally accepted that the biochemical phenotype does not allow for a reliable assessment of the risk associated with the single mutations. Insights into the molecular effects of the mutations on the corresponding protein would be helpful to estimate their pathogenic relevance. Yet, experimental data on the molecular consequences of the various novel missense mutations identified in NBS is scarce and mainly refers to the mild temperature-sensitive Y42H mutation (18,21,22). The aim of this study, therefore, was to elucidate the impact of mutations found in presymptomatic newborns on conformation, stability and catalytic function of the variant MCAD proteins.

MCAD is a member of the acyl-CoA dehydrogenase (ACAD) family of flavoproteins, which catalyzes the first step of the mitochondrial β-oxidation of medium-chain fatty acids. The ACAD family comprises nine known members, five of which are involved in fatty acid oxidation, four in amino acid oxidation (23). Each subunit of the homotetrameric MCAD enzyme is composed of three structural domains of approximately equal size, namely the N-terminal α-domain (residues 1–129), the β-domain (residues 130–239) and the C-terminal α-domain (residues 240–396). The N- and C-terminal domains predominantly consist of densely packed α-helices, which shape the core of the tetramer. The middle β-domains are exposed at the surface of the molecule and comprise two orthogonal β-sheets. The catalytic centers consisting of the binding sites for the substrate and the natural cofactor flavin adenine dinucleotide (FAD) are mainly formed by the interface between the β-domain and the C-terminal α-domain. The three-dimensional (3D) structure is a tetrahedral arrangement of a dimer of dimers with an overall diameter of ∼90Å. The interactions between the two monomers forming a dimer are extensive and involve the FAD binding site, whereas between the two dimers predominantly helix–helix interactions are found, similar to a four-helix bundle structure (23).

In this study, we characterized ten MCAD variants with single amino acid substitutions spread over the protein derived from mutations previously reported from the NBS in Bavaria, Germany, including the two prevalent mutations Y42H and K304E (3). We established a high-yield purification protocol for recombinant prokaryotic expression of wild-type and variant MCAD proteins using a maltose binding protein (MBP)-tag. The purified proteins were subsequently characterized with respect to oligomerization, enzyme kinetics, proteolytic stability, thermal inactivation and thermal unfolding. Impressively, all variants showed alterations of protein function, yet in heterogeneous ways. Catalytic function varied from high residual activity to markedly decreased activity and severe alteration of substrate affinity. We observed aggregation with partial rescue by co-overexpression of chaperonins, decreased proteolytic stability and accelerated thermal inactivation in most variants. Thermal unfolding was facilitated in all variants. Data on proteolytic and thermal stability revealed that conformational changes and destabilization are most pronounced in mutations mapping to the β-domain of the protein. These results substantiate the hypothesis of protein misfolding with loss-of-function being the common molecular basis in MCADD. The hypothesis holds true not only for the common variant K304E, but also for mutations derived from presymptomatic patients.

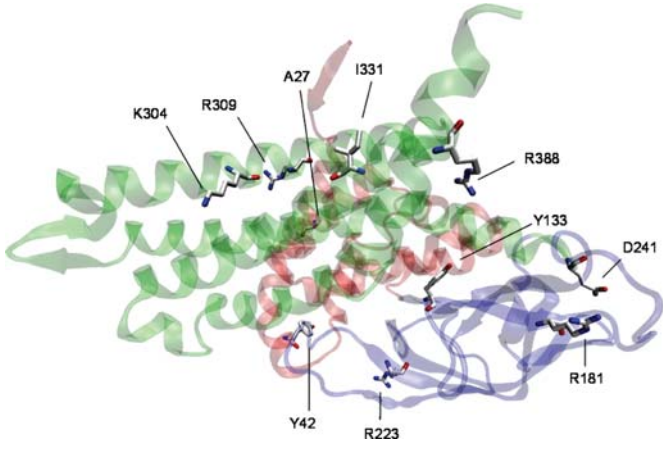

Figure 1. Structural localization of *MCAD* missense mutations analyzed. The MCAD monomer, shown as a ribbon representation, is composed of three structural domains: the N-terminal α-helix domain (residues 1–129, red), the β-sheet domain (residues 130–239, blue) and the C-terminal α-helix domain (residues 240–396, green). Amino acid residues affected by mutations are shown as stick models with carbon atoms in white, oxygen atoms in red and nitrogen atoms in blue.

RESULTS

Disturbed oligomerization is partially rescued by co-overexpression of GroESL

Wild-type and ten variant forms of MCAD (Fig. 1 and Table 1) were purified by affinity chromatography and subsequent size-exclusion chromatography (SEC) to analyze the oligomeric states of the expressed fusion proteins (Fig. 2). Wild-type MCAD was eluted in the tetrameric form with an almost negligible amount of aggregates (<1%), whereas MCAD variants showed a markedly decreased expression of soluble protein consistent with proneness to aggregation and degradation of misfolded protein. Only one variant (R388S) showed an elution profile identical to wild-type. The remaining variants revealed severely disturbed oligomerization consisting of (i) small amounts of tetramers (Y42H, D241G, R309K) with or without high molecular weight aggregates, (ii) exclusively high molecular weight aggregates (A27V, K304E, I331T) or (iii) small amounts of protein fragments of various molecular weights (Y133H, R181C) (Fig. 2A). No monomers or dimers were observed with any of the variants. R223G was expressed

Table 1. cDNA and protein location of MCAD missense mutations analyzed

cDNA[a]	Mature protein
c.155C>T	A27V
c.199T>C	Y42H
c.472T>C	Y133H
c.616C>T	R181C
c.742A>G	R223G
c.797A>G	D241G
c.985A>G	K304E
c.1001G>A	R309K
c.1067T>C	I331T
c.1237C>A	R388S

[a]Reference sequence: GenBank accession no. M16827.1. Nucleotide numbering starts with A of the ATG initiation codon as +1.

as truncated, instable protein with no detectable activity (data not shown) and could not be subjected to SEC.

Tetramer formation was partially rescued by co-overexpression of the chaperonins GroES and GroEL. Co-overexpressing GroESL, seven variants (A27V, Y42H, Y133H, R181C, D241G, K304E, R309K) showed oligomerization profiles similar to that of wild-type with only small amounts of aggregates (5–7%) (Fig. 2B). Co-overexpression of chaperonins did not enhance protein folding for the two variants I331T and R223G.

In summary, we observed disturbed oligomerization with aggregation and/or degradation in nine of 10 MCAD variants analyzed. Our results confirm that *ACADM* mutations can compromise protein folding, but misfolding can be mitigated to various extent by increasing the amount of available chaperonins.

Variant MCAD proteins show different patterns of enzyme kinetic parameters

Kinetic analyses using the ferricenium ion as an electron acceptor were performed for wild-type and purified MCAD variants (Table 2). All variants displayed Michaelis–Menten behavior. Enzyme activity with respect to V_{max} was comparable to wild-type in variants Y42H, R181C and R309K. Reduced maximal activities were found in variants A27V (38% of wild-type), D241G (48%) and K304E (46%). Variant Y133H showed the most pronounced reduction in activity (3.5%), but still followed Michaelis–Menten kinetics. V_{max} of wild-type, Y42H, and K304E are in line with the previously reported data (14,21,24).

For most of the variants, the apparent affinity to the substrate octanoyl-CoA was not or only slightly reduced. Only R388S showed an excessively decreased substrate affinity with a 100-fold increase in K_m (51.9 μM). This variant showed a 2.5-fold increase in V_{max}. However, the apparently high activity is of no physiological relevance, since it would require supraphysiological concentrations of substrate to achieve it.

K_m-values displayed in this study are 10-fold lower compared with previously reported data (14,21,24). This

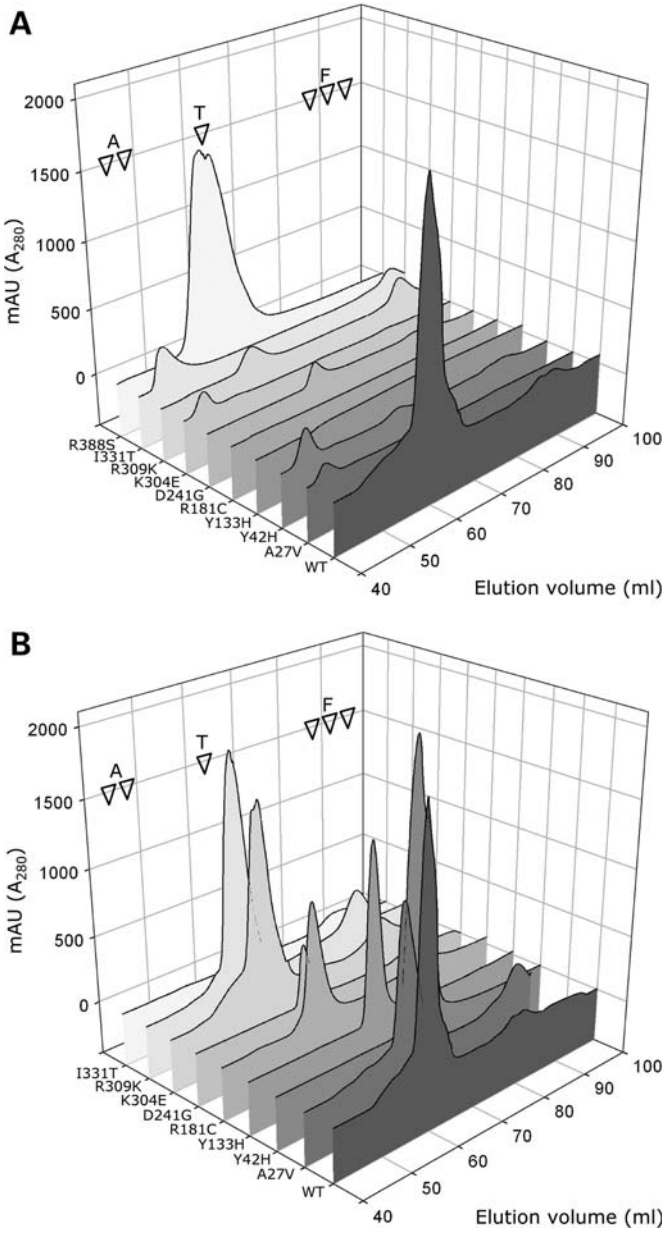

Figure 2. Disturbed oligomerization of variant MCAD proteins is partially rescued by co-overexpression of GroESL. Oligomerization profiles of wild-type (WT) and variant MCAD proteins were determined by size-exclusion chromatography. Soluble high molecular weight aggregates (A) eluted at volumes of 45–47 ml, tetramers (T) at 58–62 ml. No dimers or monomers were observed with any of the variants. Elution volumes of >85 ml contained fragments (F) of degraded MCAD or MBP. (**A**) Profiles without co-overexpression of GroESL. Wild-type (WT) and R388S almost exclusively eluted as tetramers. All other variants eluted as high molecular weight aggregates or low molecular weight fragments with only three variants (Y42H, D241G and R309K) showing small peaks of tetrameric MCAD. Aggregates and degradation products of Y133H and R181C comprised various molecular weights spread all over the chromatogram. (**B**) Profiles with co-overexpression of GroESL. Variants A27V, Y42H, Y133H, R181C, D241G, K304E and R309K showed a rescue of tetramer formation with only small amounts of aggregates. Only for variant I331T, tetramer formation could not be restored. Note: for WT, the chromatogram without co-overexpression of GroESL is depicted.

Table 2. Enzyme kinetic parameters of wild-type and variant MCAD proteins

Missense mutation	K_m (μM octanoyl-CoA)	SEM[b]	V_{max} (μmol ferricenium/min × mg protein)	SEM[b]
WT	0.4	0.04	37.1	1.49
A27V	0.5	0.11	14.1	1.16
Y42H	0.7	0.10	35.4	3.00
Y133H	0.7	0.11	1.3	0.13
R181C	0.9	0.11	41.5	0.77
D241G	0.8	0.23	17.7	1.43
K304E	0.6	0.29	17.0	2.08
R309K	0.7	0.11	32.0	0.92
R388S[a]	51.9	12.67	88.2	13.54

Steady-state kinetic parameters of wild-type (WT) and variant tetrameric MCAD proteins. Maximum activities (V_{max}) and apparent substrate affinities (K_m) of octanoyl-CoA oxidation were determined by Michaelis–Menten kinetics using a substrate range of 0–20 μM.
[a]Enzyme kinetic parameters determined at 0–150 μM octanoyl-CoA.
[b]Standard error of the mean of $n = 3$ independent experiments.

Table 3. Proteolytic stability of wild-type and variant MCAD proteins

Missense mutation	$t_{1/2}$ (min)	SEM	*P*-value	Plateau (%)	SEM	*P*-value
WT	31.2	6.6		70.1	5.8	
A27V	34.5	2.8	ns	57.6	3.7	ns
Y42H	41.2	4.0	ns	56.8	10.6	ns
Y133H	7.2	0.2	<0.05	10.0	3.6	<0.01
R181C	29.4	8.7	ns	33.4	6.0	<0.01
D241G	23.9	3.8	ns	8.2	2.5	<0.01
K304E	30.7	7.3	ns	61.6	5.0	ns
R309K	7.7	2.7	<0.05	47.6	1.9	<0.01
R388S	19.2	7.30	ns	52.3	1.2	ns

Stability of wild-type (WT) and variant MCAD proteins against limited proteolysis by proteinase K. The velocity of degradation ($t_{1/2}$) was assessed using a low protease:substrate ratio (1:25). The amount of protein not susceptible to proteolysis (plateau) was determined at a higher protease:substrate ratio (1:1). The calculated half-lives ($t_{1/2}$) are given in minutes, plateaus of degradation in per cent, both with corresponding standard errors of the mean (SEM) of $n = 3$ independent experiments. Significances for the differences between wild-type and the variants were calculated by one-way ANOVA and a Dunnett's post test. (ns, not significant).

observation might be an effect of correcting our measurements for background ferricenium reduction, correcting octanoyl-CoA concentrations for oxidizable substrate (see Materials and Methods) and optimizing the assay for sensitive and short duration measurements. However, the scale of the reported differences between K_m-values of wild-type, Y42H and K304E is well comparable.

Taken together, the MCAD variants analyzed showed different patterns of kinetic parameters: (i) activity comparable to wild-type, (ii) reduced and markedly reduced maximal activity and (iii) an excessive decrease in affinity to octanoyl-CoA as a substrate.

Susceptibility to proteinase K is increased

Limited proteolysis is used for probing protein conformation and folding kinetics. It can provide important information on local unfolding and the equilibrium between the native state oligomeric protein and its folding intermediates, since misfolded proteins are more susceptible to degradation by proteases (25). To this aim, MCAD proteins were probed with proteinase K, because its proteolysis is not limited to sequence specificity but by stereochemistry and flexibility of the protein substrate. The proteolytic stability of wild-type and variant MCAD proteins was analyzed by determination of the half-lives, indicating the velocity of degradation, and the plateaus of degradation, indicating the residual amount of protein not susceptible to proteolysis (Table 3). Five variants (Y133H, R181C, D241G, R309K and R388S) showed reduced half-lives compared to wild-type, two of which reached statistical significance (Y133H and R309K). The plateaus of degradation, however, were significantly decreased in 4 of these variants (Y133H, R181C, D241G and R309K). This finding was most pronounced in variants Y133H and D241G with residual protein amounts of 10 and 8%, respectively. Notably, the plateau of degradation of the wild-type protein was found to be 70%, indicating that at the assay conditions (37°C, 120 min) 30% of the wild-type protein is unfolded. This finding reflects the thermal sensitivity of the MCAD protein, which is additionally influenced by the protein concentrations used in the assay (21).

The decreased proteolytic stability of the variants compared to wild-type is in line with the hypothesis of an altered folding equilibrium shifted towards folding intermediates and destabilization due to local protein unfolding.

Resistance of catalytic function against thermal stress is reduced

We assessed the thermal effect on activity of wild-type and variant MCAD proteins over a range of 25–55°C. The midpoint of thermal inactivation ($T_{1/2}$), i.e. the temperature at 50% residual activity, was monitored by determination of the residual activity at different temperatures. Near the midpoint of denaturation of the wild-type (44.5°C), kinetic stability expressed as half-lives ($t_{1/2}$) was determined at 41°C (Fig. 3 and Table 4). A significant reduction of $T_{1/2}$ compared with wild-type was found in all MCAD variants analyzed except for K304E and R388S. Alterations were most pronounced in Y133H (33.6°C), R181C (34.3°C) and D241G (33.9°C). These three variants also showed significantly decreased half-lives of 6.1 min (Y133H), 6.8 min (R181C) and 9.7 min (D241G) when subjected to thermal stress as a function of time (wild-type 20.0 min). The differences among wild-type, Y42H and K304E with respect to $T_{1/2}$ are in line with the previously published data (14,18,21,26).

These observations indicate that temperature has a significant impact on catalytic function in variant MCAD proteins. Notably, these effects are detectable at physiologically relevant temperatures.

Thermal stress induces accelerated denaturation

To determine aberrant folding of MCAD with respect to ground state hydrophobicity and thermal denaturation, we performed 8-anilino-1-naphtalenesulfonic acid (ANS)

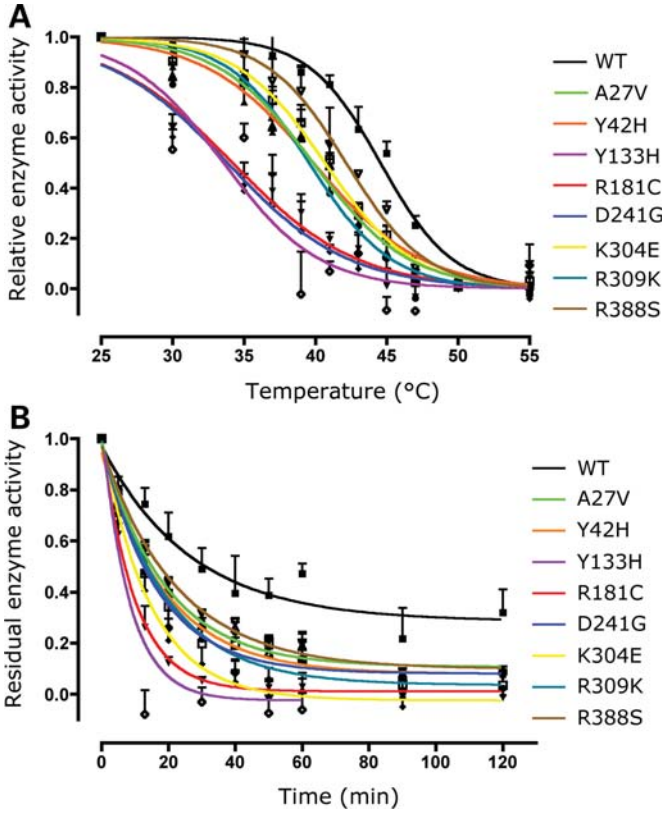

Figure 3. Variant MCAD proteins show early thermal inactivation and reduced kinetic stability. The effect of thermal stress on enzyme activity of wild-type (WT) and variant MCAD was analyzed. (**A**) Thermal inactivation profiles. Proteins were incubated at increasing temperatures (25–55°C) and the residual enzyme activities were determined. All variants showed a left-shift of the curves in comparison to WT indicating an inactivation of the enzyme at lower temperatures (Table 4, left panel). (**B**) Kinetic stability at 41°C. Proteins were incubated at 41°C and the residual enzyme activity was determined at incremental time points. For all variants, steeper slopes of the curves were observed indicating a reduction of half-lives compared with WT (Table 4, right panel). Data points of residual activities in both datasets were normalized to the initial enzyme activity and subjected to non-linear regression analysis. Error bars represent the mean ± SEM of $n = 3$ independent experiments.

Table 4. Thermal inactivation and kinetic stability of wild-type and variant MCAD proteins

Missense mutation	Thermal inactivation			Kinetic stability at 41°C		
	$T_{1/2}$ (°C)	SEM	*P*-value	$t_{1/2}$ (min)	SEM	*P*-value
WT	44.5	0.45		20.0	2.36	
A27V	39.8	0.88	<0.05	11.8	2.28	ns
Y42H	39.8	0.52	<0.05	12.7	1.35	ns
Y133H	33.6	1.01	<0.01	6.1	1.14	<0.01
R181C	34.3	1.28	<0.01	6.8	0.88	<0.01
D241G	33.9	1.08	<0.01	9.7	0.91	<0.05
K304E	40.6	0.43	ns	12.8	2.53	ns
R309K	38.8	1.80	<0.01	12.9	1.57	ns
R388S	42.0	0.37	ns	15.7	0.59	ns

Thermal inactivation and kinetic stability of wild-type (WT) MCAD were compared with variant MCAD proteins. For thermal inactivation, residual activities at different temperatures (25–55°C) were subjected to non-linear regression analysis and the midpoints of thermal inactivation ($T_{1/2}$) were calculated. $T_{1/2}$-values represent the temperature at 50% residual activity and are given in degree Celsius as means with the corresponding standard errors of the mean (SEM) of $n = 3$ independent experiments. For kinetic stability, the inactivation at 41°C was determined as a function of time. The residual activities were subjected to non-linear regression analysis and the half-lives ($t_{1/2}$) were calculated. $t_{1/2}$-values represent the time point at 50% residual activity and are given in minutes as means with the corresponding standard errors of the mean (SEM) of at least $n = 3$ independent experiments. Significances for the differences between wild-type and the variants were calculated by one-way ANOVA and a Dunnett's post test. (ns, not significant).

fluorescence experiments. The use of the hydrophobic fluorophore ANS allowed monitoring of overall unfolding events, since it binds to hydrophobic groups of the denaturing protein showing a high quantum yield in its bound state, but not when solved in aqueous buffers (27). ANS fluorescence analysis of tetrameric wild-type MCAD revealed a transition midpoint ($T_{m1/2}$) between folded and unfolded state of 52.6°C. This is in agreement with previous results obtained by circular dichroism (16).

Figure 4A shows ANS fluorescence profiles upon thermal denaturation of wild-type, K304E and two severely distorted variants. In variant Y133H, a considerably (20-fold) elevated ground state fluorescence signal at 25°C was detected in comparison with wild-type. This finding indicates an increased hydrophobicity due to partial protein unfolding even without the application of thermal stress. The same was found in R181C and K304E, but to a much lesser extent. Upon thermal denaturation, for all MCAD variants the transition from the native state to the unfolded state occurred at significantly lower temperatures than in the wild-type (Fig. 4B and Table 5). The variants Y133H and R181C showed the most pronounced alterations with $T_{m1/2}$ of 42.2 and 40.0°C, respectively. In addition to the marked left-shift of the curve, Y133H revealed a steeper slope of the curve indicating an accelerated progress of unfolding with complete denaturation at 46°C.

In summary, we observed facilitated unfolding upon thermal stress of various degrees in all variants, but also partial unfolding/misfolding in the ground state for some variants. The variant Y133H disclosed signs of severe impairment of structural integrity consistent with the findings from the other stability experiments.

Functional and conformational impact of amino acid replacements on 3D networks of side-chain interactions

Our experiments revealed severe functional and structural impairment, in particular, for the variants Y133H, R181C and R388S. To gain further insights into how these mutations exert their deleterious effects on the protein, we used a 3D structural model of the porcine MCAD tetramer to investigate, whether the amino acid residues affected are involved in networks of side-chain interactions with functional and conformational impact.

Residue Y133 maps to the β-sheet domain (residues 130–239) and is an essential part of the active site (Fig. 5A). It directly interacts with the cofactor FAD via hydrogen bond formation. Its aromatic side-chain points towards the hydrophobic core of the deep binding cavity for the fatty acid portion of the substrate establishing hydrophobic interactions with the residues L103, V135, F177, A248 and F252 which

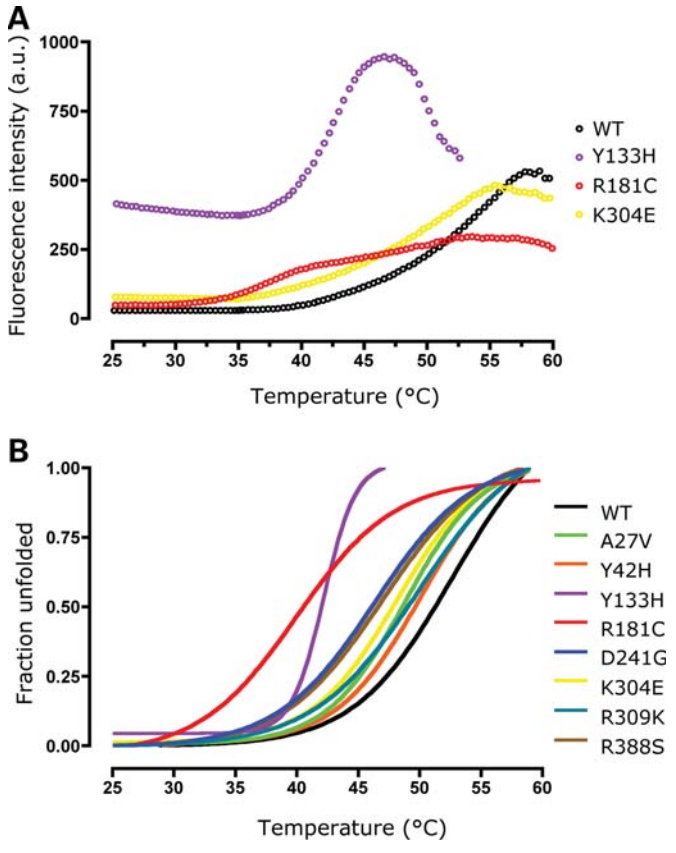

Figure 4. Variant MCAD proteins show accelerated thermal denaturation and partial protein unfolding in the ground state for some variants. Thermal unfolding of wild-type (WT) and variants monitored by ANS fluorescence. (**A**) ANS fluorescence profiles of wild-type, Y133H, R181S and K304E. Intensities of the fluorescent dye ANS, which binds to hydrophobic groups of the protein presented upon unfolding, are plotted as a function of increasing temperatures. Ground-state fluorescence was markedly increased for Y133H and, to a lesser extent, for R181C and K304E indicating an increased hydrophobicity due to partial unfolding of these variants already in the native state. (**B**) Thermal denaturation of all variants analyzed. Fractions of unfolded protein are plotted as a function of increasing temperatures and the transition midpoints represent the temperature at half denaturation (fraction unfolded 0.5). All variants showed a marked to moderate left-shift of the curves implying an increased propensity to unfold upon thermal stress (Table 5). In addition, Y133H showed accelerated unfolding as indicated by the steeper slope of the curve and complete denaturation at 46°C.

line the cavity. To poise the $C_\alpha - C_\beta$ bond of the fatty acid for dehydrogenation, it is sandwiched between the *re*-face of the isoalloxazine moiety of FAD and the catalytic base E376. A replacement of the large, hydrophobic tyrosine by the smaller, positively charged histidine is supposed to distort the hydrophobic packing of the binding cavity and by this to lead to a conformational rearrangement of the active site pocket. As a result, the correct 3D arrangement of FAD, the $C_\alpha - C_\beta$ bond of the substrate and the catalytic base E376 will be impaired leading to the marked disturbance in enzyme function. Moreover, A248 and F252 are located within the α-helix G. Interactions between α-helices G and H in one subunit of the dimer and α-helices I and K in the opposite unit of the adjacent dimer are known to promote MCAD tetramer assembly from dimers. Hence, conformational alteration of the substrate binding cavity with impairment of the helix–helix interactions due to the Y133H substitution might explain the observed distortion of the oligomeric state.

Table 5. Transition midpoints of thermal denaturation of wild-type and variant MCAD proteins

Missense mutation	$T_{m1/2}$ (°C)	SEM	*P*-value
WT	52.6	0.40	
A27V	48.8	0.69	<0.01
Y42H	50.1	0.19	<0.01
Y133H	42.2	0.11	<0.01
R181C	40.0	0.16	<0.01
D241G	46.4	0.65	<0.01
K304E	48.2	0.16	<0.01
R309K	50.0	0.14	<0.01
R388S	47.0	0.85	<0.01

Transition midpoints of thermal denaturation obtained by ANS fluorescence of wild-type (WT) MCAD were compared with variant proteins. Three sets of independent experiments were performed. The transition midpoints ($T_{m1/2}$) were calculated by non-linear regression analysis and are given in degree Celsius as means with their corresponding standard errors of the mean (SEM). Significances for the differences between wild-type and variants were calculated using one-way ANOVA followed by a Dunnett's post test.

R181 is located at the beginning of an extended loop structure (residues 181–193) at the surface of the protein that connects β-sheets 4 and 5 (Fig. 5B). The loop contributes to the crevice shaping the entrance to the active site and, due to its strong interactions with the beginning of the C-terminal α-domain, plays a pivotal role for MCAD tetramerization. R181 networks with D183, D185, K187 and A188 to poise the loop in its proper structural conformation. It is well conceivable that the severe structural distortion of the protein with reduced stability and impaired tetramer assembly shown for R181C is due to a disruption of this network caused by the replacement of arginine by a small, polar, uncharged amino acid.

R388 maps to the end of the C-terminal α-domain (residues 240–396) and is part of an interface of two subunits that define a funnel-shaped crevice, the entrance to the active site mentioned above (Fig. 5C). It is shaped by α-helix K and the loops among β-sheets 4 and 5, α-helices H and I and α-helices G and H of the adjacent subunit. R388 forms a hydrogen bond to the AMP portion of the CoA moiety and is part of a side-chain network comprising both hydrogen bonds and electrostatic interactions with the neighboring residues E389 and R324 in the loop between α-helices H and I. A substitution of the large, basic, positively charged arginine by serine might disrupt this network by introducing a gap in the 3D structure of the crevice. This conformational rearrangement at the entrance to the active site will hinder the accessibility of the substrate octanoyl-CoA and the interaction with the AMP portion of the CoA moiety. This is in line with our observation that R388S displays a significant decrease in substrate affinity for octanoyl-CoA.

DISCUSSION

NBS for MCADD has revealed an increasing number of missense mutations that have never been identified in clinically diagnosed patients and we have previously described eight